DUACS DT2021 reprocessed altimetry improves sea level retrieval in the coastal band of the European Seas

Antonio Sánchez-Román[1], M. Isabelle Pujol[2], Yannice Faugère[2], Ananda Pascual[1]

[1]Instituto Mediterráneo de Estudios Avanzados, C/Miquel Marqués, 21, 07190 Esporles, Spain
[2]Collecte Localisation Satellites, Parc Technologique du Canal, 8-10 rue Hermès, 31520 Ramonville-Saint-Agne, France

Correspondence to: Antonio Sánchez Román (asanchez@imedea.uib-csic.es)

Abstract. More than 29 years of altimeter data have been recently reprocessed by the multi satellite Data Unification and Altimeter Combination System (DUACS) and made available under the name of DT2021 processing through the Copernicus Marine Service (CMEMS) and the Copernicus Climate Change (C3S) Service. New standards have been applied and various geophysical correction parameters have been updated compared to the previous release in order to improve the product quality. This paper describes the assessment of this new release through the comparison of both *all satellites* and *two satellites* products with external in situ tide gauge measurements in the coastal areas of the European Seas for a time period spanning from 1 January 1993 to 31 May 2020. The aim is to quantify the improvements on the previous DT2018 processing version on the retrieval of sea level in the coastal zone.

The results confirmed that the CMEMS product in the new DT2021 processing version better solves the signal in the coastal band. The *all satellites* dataset showed a reduction of 3% in errors when compared with tide gauges and of 5% in the variance of the differences between the datasets compared to DT2018 reprocessing. Moreover, the *all satellites* dataset provided more accurate sea level measurements when comparing with tide gauges respect to the climatic *two satellites* dataset due to the better performance of the former for the assessment of higher than climatic frequency signals. On the contrary, the *two satellite* dataset is the most suitable product for the assessment of long-term sea level SSH trends in the coastal zone due to its larger stability to the detriment of the *all satellites* dataset.

1 Introduction

On December 2021, more than 29 years of Level 3 (L3) and Level 4 (L4) altimetry products were reprocessed, released and made freely available for users as the "DT2021" version (CMEMS-SL-QUID, 2022; C3S-PUG, 2022; Faugère et al., 2022) of the multi-satellite Data Unification and Altimeter Combination System (DUACS) products by the European Copernicus Program (http://marine.copernicus.eu/) substituting the former "DT2018" product version (Taburet et al., 2019) which is no longer available in the Copernicus Catalogue. Currently, two types of altimetric L4 gridded products generated by the DUACS production system are available: the so called *all satellites* global and regional (European Seas) gridded products disseminated via the Copernicus Marine Service (CMEMS) project (CMEMS-SL-QUID, 2022); and the *two satellites* global gridded products distributed via the Copernicus Climate Change Service (C3S) project (C3S-PUG, 2022). Currently, the *two satellites* products are also distributed via the CMEMS project. The *all satellites* products are dedicated to the retrieval of mesoscale signals on a global or regional scale whereas the *two satellites* ones are dedicated to monitoring the long-term evolution of sea level, thus being suitable for using in climate applications (Taburet et al., 2019).

The Level 2 altimeter standards used to compute sea level anomaly (SLA) in the CMEMS and C3S products are identical (CMEMS-SL-QUID, 2022), but the reference used to compute SLAs differs: CMEMS products use a mean profile of sea surface heights along the theoretical track of the satellites with a repetitive orbit, whilst C3S products use a mean sea surface (MSS) for all missions. In the latest release, new up-to-date standards have been applied and various geophysical correction parameters have been updated compared to the previous DT2018 version (Table A1 in Appendix A). This provides both an improved accuracy of SLA and lower regional sea level biases.

Namely, (i) a **new internal tide correction** that allows the prediction of the two main tidal constituents of both diurnal and semidiurnal tidal frequencies has been applied. The solution proposed by Zaron (2019) is used (HRET 8.1 version). This correction reduces the coherent signal characteristic of internal tide and provides a more precise reconstruction of mesoscale eddies. The use of the internal tide correction induces a reduction of internal tide signature on along-track data improving the precision of the resulting L4 gridded product (CMEMS-SL-QUID, 2022).

(ii) a **new MSS** for non-repetitive missions and recent missions consisting in a hybrid gridded MSS field made up of three different gridded MSS models is used. Namely, SIO MSS model (Sandwell et al., 2017) is used in open ocean, CNES_CLS-2015 model (Pujol et al., 2018) is used in coastal areas (distance to the coast lower than 20 km) and DTU15 model (Andersen et al. 2016) is used in the Arctic region (latitude larger than 80 northern degrees). This hybrid solution contributes to reduce the SLA errors at short wavelengths. A **new mean profile** (precise MSS along the altimeter tracks) is used for historical repetitive missions (CMEMS products). New mean profiles were estimated along the historical repetitive tracks of Topex/Poseidon/Jason, Topex/Poseidon/Jason-interleaved phase, ERS/Envisat/AltiKa, Sentinel-3A and GFO in consistency with the different standards used in DT2021 version. This improves the SLA signal at long wavelengths.

(iii) a **new Mean Dynamic Topography** for the Global (Mulet et al., 2021), and the Mediterranean and Black Seas is applied (Jousset et al., 2020,2022).

(iv) an **improved Long Wavelength Error (LWE) correction**, delivered in L3 product, has been computed as the final step of multi-mission cross-calibration processing. Progress with respect to the previous version has been done by first estimating the LWE correction with higher frequency along the different tracks (100 Km instead of 500 km used previously), then by improving the interpolation methodology (Optimal Interpolation instead of Spline used previously) to retrieve the correction on each along-track position. It is expected to remove local SLA residual biases between neighbouring altimeter tracks.

(v) and finally, the DT2021 products version includes an **upgraded mapping parameterisation** that contributes to improve the mesoscale signal visible on L4 products. Namely, the spatial and temporal correlation scales are optimised improving the reconstruction of the mesoscale signal, a more precise definition of the observation's errors computed with regard to the new altimeter standards is provided, and finally, a more precise estimation and correction of LWE in the mapping process is applied removing local SLA residual biases. A complete description of the different evolutions implemented in the DUACS DT2021 products version can be found in CMEMS-SL-QUID (2022).

The validation (quality check) of altimetry products is a key step in the data processing pipe to assess and characterise the errors associated with the altimetry measurements. This issue is crucial in the coastal zone, where traditional altimetry have been often unable to produce meaningful signals of sea level change due to the typically shallower water, bathymetric gradients, and shoreline shapes, among others (Vignudelli et al., 2019; Sánchez-Román et al., 2020). Actually, global and regional products from DT2021 and DT2018 reprocessings are not optimised for the coastal band promoting larger errors in the retrieval of sea level with regard to the open ocean.

Nevertheless, the monitoring of sea level changes in coastal areas is an important societal issue (Pujol et al., 2023). Thus, most of the efforts of the international community in the recent past have been focused on the research and development of techniques for coastal altimetry, with substantial support from space agencies such as the European Space Agency (ESA), the Centre National d'Études Spatiales (CNES), and other research institutions (Cipollini et al., 2017). Efforts of the coastal altimetry community are aimed at extending the capabilities of current altimeters closer to the coastal zone. This includes the application of improved geophysical corrections, data recovery strategies near the coast using new editing criteria, and high-frequency along-track sampling associated with updated quality control procedures (Vignudelli et al., 2019). As a result, regional altimeter products such as PISTACH (Mercier et al., 2010), X-TRACK (Roblou et al., 2011; Birol et sl., 2017); X-

TRACK-ALES (Birol et al., 2021) and ESA EO4SIBS (Grégoire, 2021) focused on the coastal zone have been developed over the last few years (Pujol et al., 2023). These products are disseminated to both the international scientific community and society through regular specific coastal altimetry workshops.

Different metrics are used to assess the quality of altimetry data. They mainly consist in the analysis of the SLA field at different steps of the processing; check consistency of the SLA along the tracks of different altimeters and between gridded and along-track products; and comparisons with external in situ measurements (CMEMS-SL-QUID, 2022). In situ and altimetric observations are complementary and are often assumed to observe the same signals (Wöppelmann and Marcos, 2016). In coastal areas, tide gauge measurements are commonly used. In Taburet et al. (2019), DUACS DT2018 L4 global gridded products were assessed in the coastal areas through a comparison with monthly tide gauge measurements from the Permanent Service for Mean Sea Level (PSMSL) Network (PSMSL, 2016). These authors reported a global reduction of 0.6% in variance with respect to the previous processing (DUACS DT2014 dataset). Pascual et al. (2006, 2009) investigated the consistency between previous versions of the altimeter L4 gridded products and tide gauge data from the PSMSL repository in the coastal zone reporting mean square differences between the two datasets ranging between 30% and 90% in the European coasts. More recently, Sánchez-Román et al. (2020) assessed the quality of DUACS L3 products in the coastal band of the European Seas through comparison with independent tide gauge measurements. These authors reported a mean root mean square (rms) difference between both datasets lower than 7 cm for the whole region, with mean values ranging around less than 4 cm in the Mediterranean basin and around 10 cm for the North West European Shelf (NWS) area (see Fig. 2 in Sánchez-Román et al., 2020 for the location of this region). The quality of the DUACS DT2021 product version has been also assessed through the comparison with monthly tide gauge measurements from the Global Sea Level Observing System (GLOSS)/Climate Variability and Predictability (CLIVAR) network. CMEMS-SL-QUID (2022) reports improved results when using the latest reprocessing with a reduction in variance of the differences between altimetry and tide gauges ranging between 0.2% and more than 5% of the tide gauge signal in the European coasts; with respect to the previous product version.

This paper focuses on improvements of the latest reprocessing of DUACS Delayed Time (DT) reanalysis (referred hereinafter as DT2021) in the retrieval of sea level in the coastal band of the European Seas with respect to the previously available reprocessed products (referred hereafter as DT2018). To do that, an intercomparison of L4 global altimetry gridded products and in situ tide gauges located along the European coasts from the Copernicus Catalogue is conducted. The performance of the DT2021 processing *all satellites* and *two satellites* versions on the sea level retrieval is also assessed. The paper is organized as follows: the SLA data used, the tide gauge dataset, and the method for comparing altimeter and in situ measurements are detailed in section 2. Section 3 describes the performance of the DT2021 processing product version in the retrieval of sea level in the coastal band. Also, the improvements over the previous DT2018 processing product version is assessed. Finally, the discussion and main conclusions are included in section 4.

2 Materials and methods

2.1 Sea level anomaly data

The DUACS reprocessed L4 global satellite SLA maps used in this study correspond to both the DT2021 (CMEMS-SL-QUID, 2022; C3S-PUG, 2022; Faugère et al., 2022) and DT2018 product (Taburet et al., 2019) versions. SLA gridded products cover the global ocean with a spatial and temporal resolution of ¼ of a degree and 1 day, respectively. Two different SLA datasets for each one of the DUACS product versions are considered: the *all satellites* L4 global gridded product disseminated via the CMEMS and the *two satellites* L4 global gridded product distributed via the C3S and CMEMS. The first one is computed with a satellite constellation including all the available altimeters at a given time (ranging from 2 to 7 over the period considered in this study, see e.g. Fig. 1 in Coastal Altimetry Team, 2021; Morrow et al., 2023). As a consequence, the errors are not constant in time since they depend on the number of satellites used. This product focuses on the mesoscale mapping capacity of the altimeter data together with the stability of the overall dataset. The *two satellites* SLA dataset is obtained by merging a steady number of altimeters (two) in the satellite constellation. Two satellites is the minimum requirement to retrieve mesoscale signals in delayed time conditions. (Pascual et al., 2006; Dibarboure et al., 2011). This fact also promotes nearly consistent errors during the whole time period (some variation of the error can occur related to changes of the *two satellite*s constellation). This product focuses on the stability of the global mean sea level (MSL), even if this implies potential reduction of the spatial sampling of the ocean. The reader is referred to Fig. 1 in Sánchez-Román et al. (2020) for more information about the DUACS procedure flowchart applied to the altimetry data and also to the processing of the tide gauge data used to compare with altimetry (next section). The time period investigated common to both DT2021 and DT2018 reprocessings spans from 1 January 1993 to 31 May 2020 due to the presently availability of DUACS DT2018 products. A complete description of the SLA datasets can be found in CMEMS-SL-QUID (2022).

2.2 Tide gauge observations

The sea level records used to compare with satellite altimetry were extracted from the Copernicus Catalogue (www.marineinsitu.eu). The tide gauge stations located in the European Seas' domain were initially considered for this study. Following the methodology described in Sánchez-Román et al. (2020), the quality flags of the tide gauge records were checked in order to remove observations with no quality check, potentially and bad data, and changes in the vertical reference of the tide gauge. Also, observations with values larger than three times the standard deviation of the time series were rejected as they could not be representative of ocean sea level changes but local features (e.g., river discharge, Laíz et al., 2013). The final dataset consists of 213 tide gauge stations (Fig. 1) with time series exhibiting between 90% and 100% of valid data. The stations and their information are listed in Table B1 in Appendix B.

Before they can be compared with altimeter data, tide gauge measurements have to be processed to remove oceanographic signals whose temporal periods are not resolved by altimetry, thus avoiding important aliasing errors (Vignudelli et al., 2019). We applied the methodology described in Sánchez-Román et al. (2020). In the following we summarise the corrections applied to the tide gauge records:

- **Correction of oceanic tidal effects** by filtering tidal components (mainly diurnal and semidiurnal tidal constituents). The u-tide software (Codiga, 2011) is used. The annual and semiannual frequencies, mainly driven by steric effect, are kept in the tidal residuals since they are included in the altimetry data.

- **Removal of the atmospherically induced sea level** caused by the action of atmospheric pressure and wind (Dorandeu and Le Traon, 1999; Carrère and Lyard, 2003). The same Dynamic Atmospheric Correction (DAC) as for altimetry is applied for the sake of consistency. The 6 hourly fields of this correction, available at the Archiving, Validation and Interpretation of Satellite Oceanographic Data (AVISO) website, are used. For each tide gauge site, the nearest grid point was selected and used to remove the atmospherically induced sea level from observations, previously converted into 6 hourly records (Marcos et al., 2015).

- **Correction of vertical movements** associated with glacial isostatic adjustment (GIA). GIA was considered as the only source of vertical land motions. Its effects were removed from the SSH records, previously averaged into daily data, by using the Peltier mantle viscosity model (VM2) (Peltier, 1998, 2004).

2.3 Method for comparing altimeter and in situ tide gauge records

The comparison method of altimetry with tide gauges consisted of collocating both datasets in time and space. As a first step, a 15-day low-pass Loess filter was applied to altimetry and tide gauge time series to remove the high frequencies that cannot be resolved by the altimetric data (Pascual et al., 2009; Ballarotta et al., 2019; Sánchez-Román et al., 2020). Then, the correlations between each tide gauge record and SLA time series corresponding to grid points within a radius of 1 degree around the tide gauge site were computed and the most correlated altimetry point was chosen. Only long-term monitoring stations with a lifetime of more than three years were used in order to allow statistical significance. Statistical analyses were performed using all available data pairs (altimetry-tide gauge). The collocated altimeter and tide gauge measurements were analysed in terms of the rms difference and variance of the time series. In addition, the robustness of the results was investigated according to Sánchez-Román et al. (2017, 2020) using a bootstrap method (Efron and Tibshirani, 1986), which allows us to estimate quantities related to a dataset by averaging estimates from multiple data samples. To do that, the dataset is iteratively resampled with replacement. A total of 1.000 iterations were used to ensure that meaningful statistics such as standard deviation could be calculated on the sample of estimated values, thus allowing us to assign measures of accuracy to sample estimates (Sánchez-Román et al., 2020).

3 Results

3.1 Performance of DUACS DT2021 products in the retrieval of sea level in the coastal band

This section presents the statistics of the comparisons performed between the DUACS DT2021 *all satellites* and *two satellites* datasets and the tide gauge observations from the Copernicus catalogue in the coastal region of the European Seas in terms of errors (rms differences) and variance of the differences between the datasets. According to Sánchez-Román et al. (2020), the bootstrapping technique was applied to gain an estimation of the standard errors of the differences between the datasets.

The mean value of the rms difference between the *all satellites* dataset and tide gauges is 4.11 cm, the variance of the differences (altimetry–tide gauge) is 17 cm^2, and the mean distance between the location of the tide gauge and the corresponding altimeter data with the highest correlation is 82 km (Table 1). These values raise to 4.35 cm, 19 cm^2, and 87 km, respectively, when using the *two satellites* dataset. The tide gauge stations (213 stations) common to both datasets were used. Thus, the *all satellites* dataset reduces the rms differences with tide gauges in the European coasts by 5%, the variance differences between the datasets by 10% and the mean distance between the most correlated altimetry point and tide gauges by 6%. Also, the number of valid data pairs used to conduct the intercomparison enhanced by 0.2% when using the *all satellites* dataset. This is due to the larger number of satellite missions used to generate this dataset, that provides lower errors in the optimal interpolation procedure compared to the *two satellites* dataset.

Table 1. Intercomparison of DUACS DT2021 satellite altimetry (ALT) and tide gauge (TG) data from the European coasts in terms of the rms differences (cm) and variance (cm^2) of the differences between the datasets. The number of tide gauge stations used in the comparison, the mean distance between tide gauges and the most correlated gridded altimetry points, and the number of total data pairs (altimetry-tide gauge) used in the computation are displayed. The common tide gauge stations for the *all satellites* and *two satellites* datasets were used. Values in parenthesis show the uncertainties (error bars) computed for the rms differences and variance from the bootstrap method using 1.000 iterations. Finally, the improvement (%) of the *all satellites* dataset in comparison with tide gauges in terms of lower rms differences, lower variance of the differences (altimetry-tide gauge), and lower mean distance between the most correlated altimetry point and tide gauges with respect to the *two satellites* dataset is also displayed.

DUACS DT2021	*all satellites* dataset	*two satellites* dataset	*all satellites* improvement
rms diff. (cm)	4.11 (0.01)	4.35 (0.01)	5 %
var TG (cm^2)	89 (1)		
var ALT (cm^2)	81 (1)	79 (1)	
var TG-ALT (cm^2)	17 (1)	19 (1)	10 %
data pairs	1.163.588	1.161.315	0.2 %
stations	213		
Distance TG (km)	82	87	6 %

Fig. 1 shows the consistency between the DUACS DT2021 *all satellites* dataset and the tide gauge data computed from Eq. (1) in Sánchez-Román et al. (2020). Consistency is expressed as the mean square differences between both datasets, computed as the variance of the differences (altimetry–tide gauge), in terms of percentage of the tide gauge variance. Overall, mean square differences lower than 5 % are observed in the central and eastern parts of the Baltic Sea, emphasising the precision of the corrections applied to the altimeter data in the basin; whereas they reach values between 20% and 30% for stations located in the connection region with the North Atlantic Ocean. The mean square differences are between 20% and 50% for most of the stations located along the Atlantic shore, this including the Strait of Gibraltar area. Such large error could be related to imprecisions of the correction applied (i.e. ocean tide and DAC) to the altimeter data (Pascual et al., 2008; Laíz et al., 2016; Sánchez-Román et al., 2020), and also to both the larger spatiotemporal variability observed in this region (figure not shown), and to a larger non tidal variance with respect to that found in the Baltic Sea (Von Schuckmann et al., 2018). Finally, the Mediterranean and Norwegian Seas show mean square differences ranging between 15% and 30%, except for the Balearic Islands (western Mediterranean) and the southwestern part of Norway where values between 5% and 15% are obtained. The consistency between the DUACS DT2021 *two satellites* dataset and tide gauges (figure not shown) presents a quite similar spatial pattern and results. These outcomes improve the ones reported in Sánchez-Román et al. (2020) from the intercomparison conducted between Sentinel-3A L3 along track DUACS DT2018 dataset and tide gauge measurements in the region computed over a period of two and a half years.

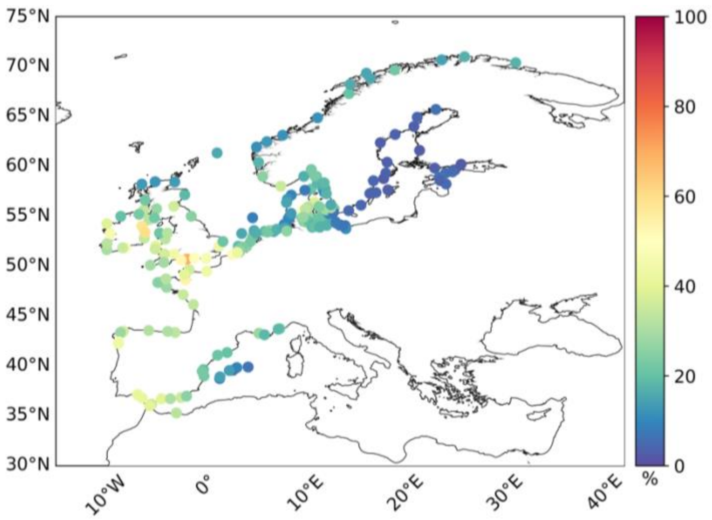

Figure 1. Location of the 213 tide gauges of the global product in the Copernicus catalogue along the European coasts and the western Mediterranean Sea used to compare with altimetry data after applying the selection criteria described in the text. Colours indicate the mean square differences between the tide gauge and altimetry sea level (DT2021 *all satellites* series). Units are the percentage of the tide gauge variance.

3.2 Improvement of DT2021 over DT2018 reprocessing

3.2.1 *all satellites* SLA dataset

This section focuses on the statistics of the comparisons performed between the DUACS DT2021 and DT2018 reprocessing *all satellites* datasets and the tide gauge observations. The mean value of the rms difference between the DT2018 processing dataset and tide gauges is 4.22 cm, the variance of the differences (altimetry–tide gauge) is 18 cm^2, and the mean distance between the location of the tide gauge and the corresponding altimeter data with the highest correlation is 88 km (Table 2).

Overall, these values are larger than those reported in the previous section for the comparison using the DT2021 processing dataset (see Table 1). As a consequence, the DT2021 *all satellites* dataset reduces (i) the errors with tide gauges in the European coasts by 3%, (ii) the variance of the differences between the datasets by 5%, and (iii) the mean distance between the most correlated altimetry point and tide gauges by 7%. Also, the number of valid data pairs used to conduct the intercomparison is enhanced by 0.1% when using the DT2021 processing *all satellites* dataset. This highlights the impact of the new DUACS DT2021 reprocessing on the coastal areas, that provides more valid measurements, located closer to the tide gauge sites, compared to DT2018 reprocessing.

Table 2. The same as Table 1 but for the intercomparison using the DUACS DT2018 reprocessing. The improvements (%) of the DUACS DT2021 reprocessing *all satellites* and *two satellites* SLA datasets with respect to the previous DT2018 reprocessing are also shown.

DUACS DT2018	***all satellites* dataset**	***two satellites* dataset**	***all satellites* DT2021 improvement**	***two satellites* DT2021 improvement**
rms diff. (cm)	4,22 (0,01)	4,41 (0,01)	3 %	1 %
var TG (cm^2)	89 (1)			
var ALT (cm^2)	80 (1)	78 (1)		
var TG-ALT (cm^2)	18 (1)	19 (1)	5 %	no improvement
data pairs	1.162.231	1.161.349	0,1 %	no improvement
stations	213			
Distance TG (km)	88	90	7 %	3 %

The new standards and updated geophysical corrections applied to the DUACS DT2021 reprocessing compared to the previous DT2018 version have a direct impact on the observation of coastal ocean sea level in the gridded products. To characterise this impact, the difference between DT2021 and DT2018 consistency is shown in Fig. 2. The spatial distribution of the differences in consistency shows an overall better performance of the DT2021 reprocessing (blue colours) at the connection region between the Baltic Sea and the eastern North Atlantic Ocean and in most of the Atlantic shore, where an improvement larger than 15% is found for some tide gauge sites. A degradation of the DT2021 reprocessing is observed in most of the stations located in the western Mediterranean Sea and the southern coasts of Spain, including the Strait of Gibraltar area, and also in some stations located in the coasts of France, England and Ireland. On the other hand, discrepancies are hardly observed between the two reprocessings in the Baltic and Norwegian Seas.

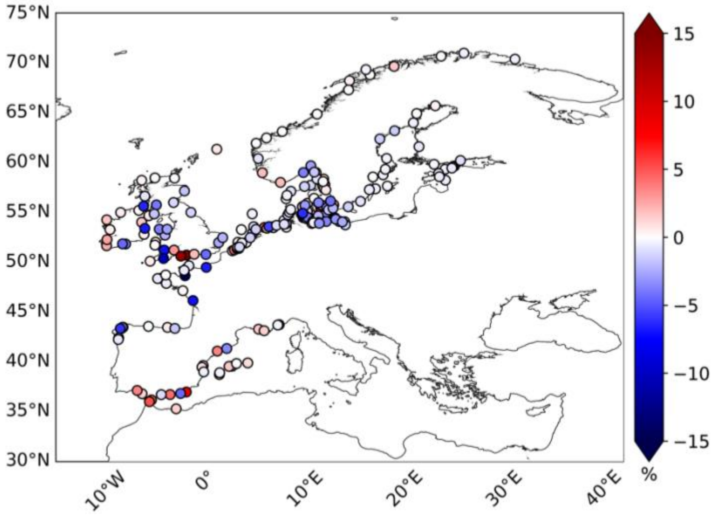

Figure 2. Spatial distribution of the differences (DT2021 minus DT2018) for the mean square differences between the tide gauge and altimetry sea level. Units are the percentage of the tidal variance. The SLA *all satellites* dataset has been used. Blue colours denote an improvement of the DUACS DT2021 reprocessing whilst red colours indicate its degradation with respect to the DT2018 reprocessing.

3.2.2 *two satellites* SLA dataset

We present here the statistics of the intercomparison between the climatic (two satellites) DT2021 and DT2018 processing and tide gauges. The mean value (Table 2) of the rms difference between the DT2018 processing dataset and tide gauges is 4.41 cm, the variance of the differences (altimetry–tide gauge) is 19 cm^2, and the mean distance between the location of the tide gauge and the corresponding altimeter data with the highest correlation is 90 km. If these results are compared with those reported above for the comparison using the DT2021 processing dataset (Table 1), it can be observed that the latter only improves the previous DT2018 reprocessing in terms of the errors with tide gauges, that are reduced by 3%, and the mean distance between the most correlated altimetry point and tide gauges, reduced by 7%; whereas the variance of the differences between the datasets and the number of valid data pairs used to conduct the intercomparison are quite similar. Such improvements are around 60% lower than those reported for the *all satellites* datasets. This fact is reflected in the spatial distribution of the differences between DT2021 and DT2018 consistency with tide gauges (figure not shown). A better performance of the DT2021 reprocessing is obtained at the connection region between the Baltic Sea and the eastern North Atlantic Ocean and in part of the Atlantic shore (coasts of United Kingdom and France). There is a degradation of the DT2021 reprocessing in most of the stations located in the western Mediterranean Sea and the southern coasts of Spain; and in some stations located in the coasts of France, England and Ireland. Also, negligible discrepancies between the two reprocessings are found in the Baltic Sea. This spatial pattern is quite similar to that obtained for the *all satellites* dataset described above. However, a degradation of the DT2021 reprocessing is observed in most of the stations located in both the NWS region (southern coasts of the North Sea) and the Norwegian Sea. This is a novelty with respect to the previous computation emphasising the overall poorer improvements of the DUACS DT2021 *two satellites* dataset over the previous reprocessing.

3.2 Performance of DT2021 reprocessing in monitoring the long term evolution of sea level

The computation described above has been conducted by using all available information from the tide gauge dataset, thus including time series of different length spanning from few years to less than three decades (Table B1 of Appendix B). To assess the performance of DUACS DT2021 processing version in monitoring the long-term evolution of sea level in the coastal zone of the European Seas the analyses described above were repeated for a specific time period spanning 20 years: from 1 January 2000 to 31 December 2019. This time period has been chosen because of the largest number of available altimeter missions used to generate the *all satellites* SLA maps. Tide gauge time series with valid data within such time interval were considered; this allowing the intercomparison altimetry–tide gauges for long-term time series with the same length. Moreover, only tide gauge time series with at least 99% of valid data were used in order to allow the analysis of linear trends. This reduced the original tide gauge dataset to a subset of 27 stations (Tables B1, B2 of Appendix B) mainly located in the northern half of the Baltic Sea (70% of stations) with sparse stations distributed along the coasts of France and Spain (Fig. 3). This analysis has also been conducted for the DUACS DT2018 reprocessing for comparison purposes.

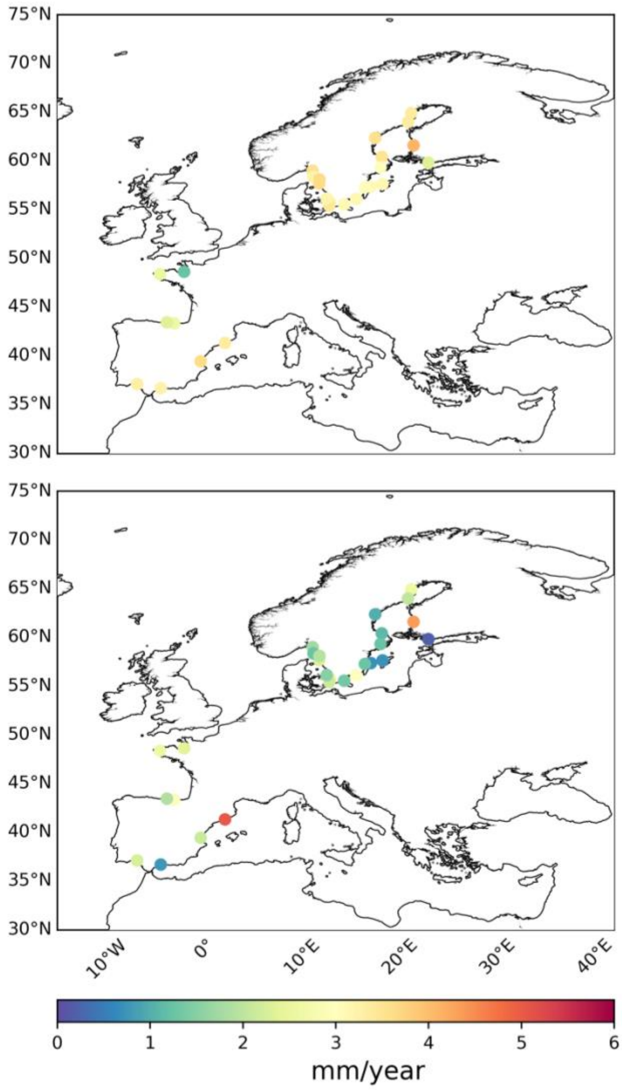

Figure 3. Spatial distribution of linear trends (mm year^{-1}) for altimetry (upper panel) and tide gauges (lower panel) computed from monthly averaged data for the 20 year time period spanning from 1 January 2000 to 31 December 2019. The *all satellites* dataset from the DUACS DT2021 reprocessing has been used.

Linear trends based on monthly observations at each tide gauge site (Fig. 3 and Table B2 of Appendix B) computed from DUACS DT2021 *all satellites* dataset (upper panel) show a homogeneous spatial pattern with overall values varying from 2.30 to 4.10 mm year^{-1} in the Baltic and Mediterranean Seas and between 2.30 and 3.30 mm year^{-1} in the sparse stations located along the North Atlantic European shore, except for the station of SaintMalo that presents a linear trend of 1.26 mm year^{-1}. Linear trends computed from tide gauges (lower panel) exhibit a more heterogeneous spatial pattern with values ranging between less than 1 mm year^{-1} for some stations located in the Baltic Sea, and 5.06 mm year^{-1} for the station of Barcelona (western Mediterranean Sea). However, most of the tide gauge stations present trend values ranging from 1.30 to 3 mm year^{-1}. These results provide further evidence, if needed, of the European Seas coastal sea level rise, including the westernmost part of the Mediterranean Sea. The differences in trends between the two datasets vary, in absolute values, between near 0 mm year^{-1} (Brest station, Atlantic French coast) to close to 2.60 mm year^{-1} found in the station of Spikarna (Baltic Sea).

Linear trends computed from DUACS DT2021 *two satellites* dataset (figure not shown) exhibit a quite similar spatial pattern with values ranging from 2.60 to 3.80 mm year^{-1} in the Baltic and Mediterranean Seas; and between 2.40 and 3.40 mm year^{-1} along the North Atlantic European coasts. However, some discrepancies between the two datasets are observed. These differences, computed as *all satellites* minus *two satellites* datasets, are displayed in Fig. 4. Overall larger linear trends (up to 1 mm year^{-1}) were obtained for the *all satellites* dataset in the northernmost and central Baltic Sea as well as in the stations located in the Mediterranean Sea whilst lower values of the same magnitude are mainly observed at the entrance of the Baltic Sea and in most of the stations located along the North Atlantic European shore.

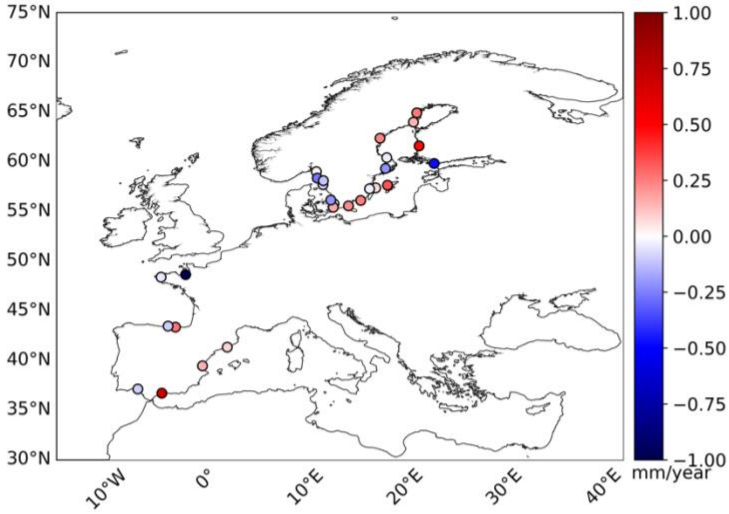

Figure 4. Spatial distribution of the differences (*all satellites* minus *two satellites* datasets) for the linear trends (mm year^{-1}) from altimetry computed from monthly averaged data for the 20 year time period spanning from 1 January 2000 to 31 December 2019. The DUACS DT2021 processing version has been used. Blue (red) colours denote lower (larger) trends for the *all satellites* dataset.

On the other hand, linear trends computed from the DT2018 reprocessing (figures not shown) exhibit a quite similar spatial pattern than that reported for the DT2021 processing version with overall values ranging from 2.20 (2.40) to 4.35 (3.60) mm year^{-1} in the Baltic and Mediterranean Seas and between 2.40 (2.10) and 3.05 (2.85) mm year^{-1} along the North Atlantic European coasts for the *all satellites* (*two satellites*) dataset. Thus, hardly any differences in range are observed between the *all satellites* dataset from the two reprocessing whereas these differences increase for the *two satellites* dataset with a lower variability observed for the DT2018 reprocessing. This fact has an impact on the spatial distribution of the differences between the two processing versions (Fig. 5).

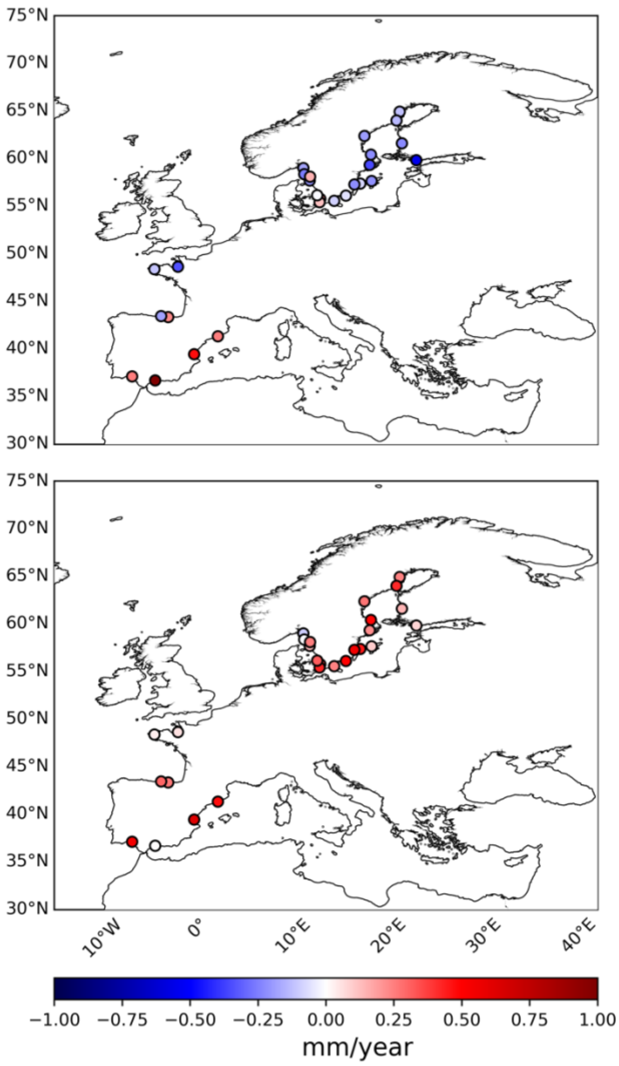

Figure 5. Spatial distribution of the differences (DT2021 minus DT2018 reprocessing) for linear trends (mm year $^{-1}$) for altimetry computed from the *all satellites* dataset (upper panel) and the *two satellites* dataset (lower panel). Monthly averaged data for the 20-year time period spanning from 1 January 2000 to 31 December 2019 has been used. Blue (red) colours denote lower (larger) trends for the DT2021 reprocessing.

For the *all satellites* dataset (upper panel in Fig. 5), two different spatial patterns were observed with lower trends for the DT2021 reprocessing in the Baltic Sea basin and most of the stations located along the North Atlantic European coasts; whereas lager values are obtained for the tide gauge stations located in the western Mediterranean Sea and some sparse stations at the entrance of the Baltic Sea. On the contrary, the spatial distribution of the differences between the two reprocessing for the *two satellites* dataset (lower panel in Fig. 5) depicts a homogeneous spatial pattern with overall larger trends for the DT2021 reprocessing except for the tide gauge station of Barseback located in the connection region between the Baltic Sea and the eastern North Atlantic Ocean (Table B2 in the Appendix B). Fig. 5 also reveals the differences between the two reprocessing, and for the two datasets, when comparing with linear trends from tide gauges: the *two satellites* dataset from the DT2021 processing version presents larger differences with tide gauges with respect to the DT2018 reprocessing in the whole domain, whilst this is only observed for sparse stations along the North Atlantic shore and the stations located in the Mediterranean Sea for the *all satellites* dataset. Thus, closer results were obtained from the DT2021 *all satellites* product with respect to the former DT2018 processing version in most of the Baltic Sea region and the stations located along the North Atlantic European coast.

4 Discussion and conclusions

More than 29 years of DUACS Level 3 and Level 4 altimeter data have been recently reprocessed and delivered under the name of DT2021 processing version through the Copernicus Marine Service and the Copernicus Climate Change Service. The *all satellites* SLA products include all the available altimeter missions (ranging from 2 to 7 over the period considered in this study), which makes the errors not constant in time since they depend on the number of satellites used. Maps from the *all satellites* products provide the most accurate sea level estimation with the best spatial and temporal sampling of the ocean at all times. The *two satellites* SLA dataset is obtained by merging a steady number of altimeters (two) in the satellite constellation. This promotes consistent errors during the whole time period. Maps that include only two satellites are used to compute the most homogeneous and stable sea level record over time and space. Thus, *two satellites* products are dedicated to monitoring long term sea level evolution for climate applications and analysing ocean–climate indicators such as global and regional MSL evolution (Taburet et al., 2019).

The new standards applied to the DT2021 version and the update of various geophysical correction parameters compared to the previous release improved the *all satellites* product quality having a direct impact on the observation of coastal ocean sea level in the gridded products. To achieve independent comparisons, SLA from altimetry in the coastal zone of the European Seas were examined through comparison with in situ tide gauge measurements. Compared to the previous DT2018 version, an improvement in the *all satellites* dataset was obtained, with a reduction of 3% in errors when compared with tide gauges and of 5% in the variance of the differences between the datasets. The mean distance between the most correlated altimetry point and tide gauges reduced by 7%. Also, the number of valid data pairs used to conduct the intercomparison enhanced by 0.1% when using the DT2021 processing. This highlights the impact of the new DUACS DT2021 version on the coastal areas, that provides more valid measurements and located closer to the tide gauge sites, compared to DT2018 reprocessing. On the other hand, almost no improvement of the DT2021 *two satellites* dataset over the previous reprocessing was found when using all available information from the tide gauge dataset (time series of different length) in the computation: errors with tide gauges were reduced by 1%, and the mean distance between the most correlated altimetry point and tide gauges was reduced by 3%. The variance of the differences between the datasets and the number of valid data pairs used to conduct the intercomparison were quite similar among the DT2021 and DT2018 processing versions. These improvements were around 60% lower than those reported for the *all satellites* datasets. This fact could be explained by differences in the mapping parameters used for the two products: DT2021 mapping parameters (i.e., spatial and temporal correlation scales, a priori errors on the measurements) are evolved in CMEMS products (CMEMS QUID, 2022) with the objective to better retrieve mesoscale signals, whilst no evolution of the mapping parameter was implemented in C3S DT2021 product (C3S PUG, 2022).

The quality assessment of DUACS DT2021 reprocessing revealed a better performance of the *all satellites* products in the retrieval of SSH in the coastal zone with respect to the *two satellites* products for the time period investigated (27 years). Namely, a reduction of 5% in errors with tide gauges and 10% in variance difference between altimetry and tide gauges was obtained when using the *all satellites* dataset with respect to the *two satellites* product. This is because despite the larger stability of the *two satellites* dataset, this product is optimised for climatic signal when analysing low frequency signals (SSH trends). Thus, it is less performant for higher frequency signals. In this context (analysis of high frequency signals), the results reported here show that the *all satellites* dataset should be considered for the analysis of long time series of SSH in the coastal zone of the European Seas including all frequency signals. This can be clearly seen in Fig. 6 showing the differences (computed as *all satellites* minus *two satellites* datasets) for consistency between altimetry and tide gauges.

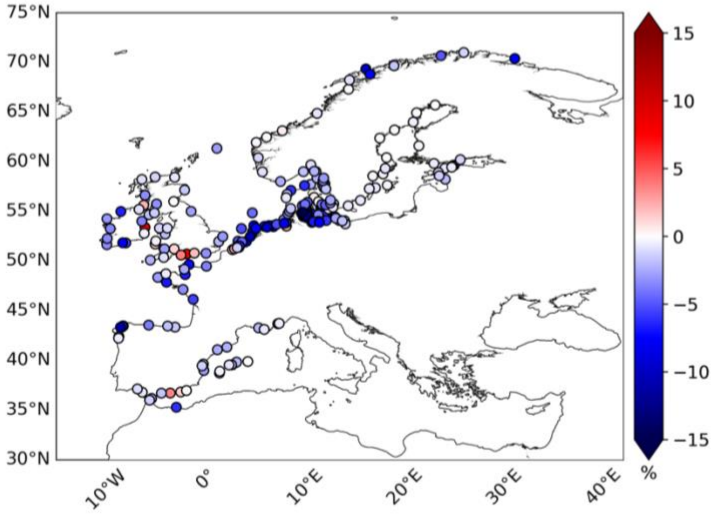

Figure 6. Spatial distribution of the differences (*all satellites* minus *two satellites* datasets) for the mean square differences between the tide gauge and altimetry sea level. Units are the percentage of the tidal variance. The DUACS DT2021 processing version has been used. Blue (red) colours denote an improvement (degradation) of the *all satellites* dataset.

An overall better performance (blue colours) of the *all satellites* product with respect to the *two satellites* one was observed in the whole domain except in the Baltic Sea and the westernmost part of the Norwegian Sea, where similar results are obtained. The improvement is larger in most of the Atlantic shore, namely at the connection region between the Baltic Sea and the eastern North Atlantic Ocean, the NWS region and the northern Norwegian Sea, with a reduction in the variance difference between the two datasets larger than 15%. The Mediterranean Sea and the Strait of Gibraltar area show closer values between the two products with an improvement lower than 5%. These improvements could be explained by the better sampling of high frequency signal in the coastal zone in *all satellites* dataset due to the large number of altimeters available to generate the SLA maps compared to the *two satellites* maps. Improved mapping parameters for mesoscale (and thus high frequency) processes could also contribute. The observed degradation of the *all satellites* product with respect to the *two satellites* one at some tide gauge sites could be due to high-frequency local features badly captured by the *all satellites* product that translate in larger errors when comparing with tide gauges.

Linear trends based on monthly observations at each tide gauge site were computed to assess whether the DUACS DT2021 release can be representative of the local sea level along the European coasts and western Mediterranean Sea. To do that, sea level linear trends for the period 2000-2019 were computed from both the *all satellites* and *two satellites* datasets. The analysis was repeated for the DT2018 reprocessing to have a term of comparison. A homogeneous spatial pattern with overall values ranging from 2.30 (2.40) to 4.10 (3.80) mm year^{-1} was obtained for the *all satellites* (*two satellites*) dataset from the DT2021 reprocessing. This promotes a mean trend for the whole domain of 3.14 (3.13) mm year^{-1}. These trends slightly differ from those computed from the tide gauge subset covering the 20 year time period, that show values ranging between less than 1 to 5.06 mm year^{-1}; the mean trend for the whole domain is 1.96 mm/year.

Thus, trends computed from DT2021 products are on average around 1.2 mm year^{-1} larger than those obtained from tide gauges. Similar overestimations in altimetry mean trends were reported by Agha-Karimi et al. (2021) in the Baltic Sea for datasets covering the time period spanning between 1993 and 2020. These discrepancies could be attributed to the heterogeneous distribution of both datasets and also the crustal land uplift due to postglacial rebound resulting from the last glacial age affecting the Baltic Basin, where most of the tide gauge stations are located. This translates in altimetry conventional measurements being not accurate enough in the coastal zone. On the other hand, when using the former DUACS DT2018 processing version slightly larger discrepancies with tide gauges were obtained for the *all satellites* dataset, with a mean trend of 3.18 mm $year^{-1}$; whilst the *two satellites* product showed closer values to tide gauges with a mean linear trend of 2.85 mm $year^{-1}$.

Overall, linear trend differences (altimetry – tide gauge) for the DT2021 reprocessing varying, in absolute value, from 0.16 to 2.57 mm $year^{-1}$, in an average of 1.43 mm $year^{-1}$ were obtained for the *all satellites* dataset. They varied from 0.03 to 2.65 mm $year^{-1}$, in an average of 1.40 mm $year^{-1}$ for the *two satellites* dataset. These discrepancies are lower than 1.5 mm $year^{-1}$ in average and corroborate the agreement and complementarity of the two techniques to measure sea level variability in the coastal zone. They also emphasise a better performance of the C3S DT2021 dataset in the estimation of sea level linear trends in the coastal zone. This was also corroborated by the computation conducted for the DT2018 reprocessing: lower differences between tide gauge and altimetry trends computed from the *two satellites* dataset were obtained. Fig. 7 displays the spatial distribution of the differences in trend computed as altimetry minus tide gauges for the *two satellites* dataset from the DT2021 reprocessing. An overall overestimation of trends from altimetry in the whole domain was obtained. On the contrary, three tide gauge sites: Bilbao in the Atlantic Spanish coast, Pori at the eastern side of the Baltic Sea, and Barcelona in the western Mediterranean Sea (Table B2 in Appendix B) showed a long-term sea level linear trend 0.58, 0.70 and 1.81 mm $year^{-1}$ larger, respectively, than that found for the closest altimetry point with the largest correlation. The differences in trend could be attributed to the aforementioned reasons rendering altimetry measurements being not accurate enough in the coastal zone. In any case, the linear trends for the tide gauge of Barcelona described above are of the same order of magnitude than those reported by Taibi and Haddad (2019) computed for the time period spanning from 1993 to 2015 (linear trend of 2.74 mm $year^{-1}$ for altimetry; 6.73 mm $year^{-1}$ for the tide gauge; trend difference of 3.99 mm $year^{-1}$), thus supporting the results obtained here.

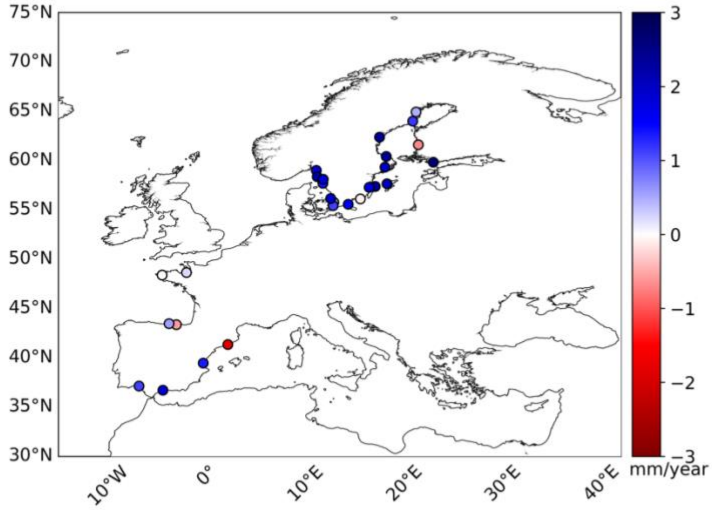

Figure 7. Spatial distribution of the differences in linear trends (mm $year^{-1}$) between the altimetry and tide gauge sea level computed for the 20 year time period spanning from 1 January 2000 to 31 December 2019. The *two satellites* dataset from the DUACS DT2021 reprocessing has been used. Blue (red) colours denote a larger (lower) altimetry linear trend.

The intercomparison conducted here between L4 gridded products from the new DUACS DT2021 release and the DT2018 version previously available; and tide gauges have demonstrated the better performance of the new DT2021 version in the retrieval of sea level in the coastal zone of the European Seas. Furthermore, the *all satellites* dataset provided more accurate sea level measurements when comparing with tide gauges respect to the climatic *two satellites* dataset due to the better performance of the former for the assessment of higher than climatic frequency signals. On the opposite, when analysing linear trends from 20-year long time series the *two satellite* dataset was the most suitable product for the assessment of long-term sea level SSH trends in the coastal zone due to its larger stability to the detriment of the CMEMS *all satellites* dataset.

SLA and derived geostrophic velocities from altimeter data have been widely compared with in situ multiplatform measurements by the coastal altimetry community in order to both validate altimetry measurements and demonstrate their capabilities to monitor sea level and surface currents in the coastal zone. Heslop et al (2017) provided the first multiplatform evaluation evolving data from the Sentinel-3A altimeter in the Balearic Sea (Western Mediterranean Sea). Their outcomes demonstrated the capacity of this satellite mission to retrieve fine-scale oceanographic features of around 20 km of diameter showing differences between along-track absolute dynamic topography (ADT) from altimetry and glider derived dynamic height (DH) data along the satellite track of 1.23 cm. In the same region, Aulicino et al. (2018) compared along-track ADT data from the SARAL-AltiKa mission with glider derived DH along two satellites tracks. They found a very similar spatial pattern with differences ranging between 1.10 and 2.90 cm. Pascual et al., (2015) also conducted an assessment of SARAL/AltiKa data in the coastal band through the comparison of along-track surface derived geostrophic velocities with surface velocities from a coastal high-frequency (HF) radar system installed in the Ibiza Channel (Balearic Sea). These authors found that the velocities derived from altimetry solved the general mesoscale features in the region with rms differences with the in situ measurements of 13 cm s^{-1}.

The new Surface Water and Ocean Topography (SWOT) satellite mission, launched in December 2022, is considered to be the next major breakthrough in satellite ocean observation (Morrow et al., 2023). The SWOT mission aims to provide SSH measurements in two dimensions along a wide-swath altimeter track with an expected effective resolution down to wavelengths of 15–30 km (Barceló-Llull et al., 2021). Thus, SWOT observations will fill the gap in our knowledge of the 15–150 km 2D SSH dynamics (Morrow et al., 2019) allowing, in some regions, the observation of the full range of mesoscale features. The assessment of their impact on the large scale ocean circulation and climate system will be one of the major challenges for the next decade.

Appendix A

Table A1. Altimeter standard used in DT2021 release. Changes with the DT2018 reprocessing are highlighted in bold format.

	TP	**Jason 1**	**Jason 2**	**Jason 3**	**ERS-1**	**ERS-2**	**ENVISAT**	**SARAL**	**Sentinel 3A**	**Sentinel 3B**	**Geosat FO**	**Cryosat 2**	**HY 2A**	**HY-2B**
ORBIT	**GSFC STD 18**	POE-E	**POE-F**		Reaper		**POE-E**	**POE-F**	**POE-F**		GSFC	**POE-F**	POE-D	**POE-F**
IONOSPHERIC	Filtered dual-frequency altimeter range measurements (Ablain and Legeais, 2010); DORIS on Poseidon		Filtered dual-frequency altimeter range (Ablain and Legeais, 2010) from SSB C-band)	Filtered dual-frequency altimeter range measurements (Ablain and Legeais, 2010)	Reaper NIC09 model (Scharroo and Smith, 2010)	**GIM** (Iijima et al., 1999)	**Filtered from L2; c>65: GIM** (Iijima et al., 1999) **corrected from 8mm bias**	GIM (Iijima et al., 1999	**Filtered from L2**		GIM (Iijima et al., 1999			**GIM** (Iijima et al., 1999
SEA STATE BIAS	Non parametric (Tran et al., 2010) on Topex; BM4 on Poseidon	2D Non parametric (Tran, 2015)	Non parametric (Tran et al., 2012)	Non parametric (Tran et al., 2012)	BM3 (Gaspar and Ogor, 1994)	Non parametric (Mertz et al., 2005)	**2D Non parametric** (Tran, 2017)	**Non parametric** (Tran, 2019)	**Non parametric** (Tran, 2012)		Non parametric (Tran, 2010)	**2D Non parametric (baseline C)**(Tran, 2018) **Baseline C**	Non parametric (Tran, 2012)	**From L2 product**
WET TROPOSPHERE	GPD+ (Ferrandes et al., 2015)	JMR (GDRE) radiometer	**AMR radiometer**		GPD+ (Ferrandes et al., 2015)		**MWR radiometer reprocessed**	**Neuronal Network (5 entries) V4**	MWR 3 radiometer		GFO Radiometer and ECMWF model	**GPD+** (Fernandes Lázaro, 2016)	ECMWF model	**ECMWF model**
DRY TROPOSPHERE	**ERA (1-hour) model based**													
OCEAN TIDE	**FES 2014 B** (Carrere et al., 2016)													
POLE TIDE	(Desai et al., 2015)**; Mean Pole Location 2017** (Ries and Desai, 2017)													
SOLID TIDE	Elastic response to tidal potential (Cartwright and Tayler, 1971; Cartwright and Edden, 1973)													
INTERNAL TIDE	**(Zaron, 2019) (HRETv8.1 tidal frequencies: M2, K1, S2, O1)**													
MEAN DYNAMIC TOPOGRAPHY	**MDT CNES_CLS_2018** (Mulet et al., 2021) **merged with regional MDT CMEMS_2020 Mediterranean and Black Sea** (Jousset and Mulet, 2020; Jousset et al., 2022)													

	TP	Jason 1	Jason 2	Jason 3	ERS-1	ERS-2	ENVISAT	SARAL	Sentinel 3A	Sentinel 3B	Geosat FO	Cryosat 2	HY 2A	HY-2B
DYNAMICAL ATMOSPHERIC CORRECTION	TUGO High frequencies forced with analysed ERA 5 pressure and wind field + inverse barometer Low frequencies		TUGO HF forced with analysed ERA 5 pressure and wind field; and after 02/2016 MOG 2D HF forced with analysed ECMWF pressure and wind field + inverse barometer LF	MOG 2D HF forced with analysed ECMWF pressure and wind (Carrère and Lyard, 2003) (operational version 3.2.0) + inverse barometer LF	TUGO High frequencies forced with analysed ERA 5 pressure and wind field + inverse barometer Low frequencies			TUGO HF force d with analysed ERA 5 pressure and wind field; and after 02/2016 MOG2D HF forced wit h analysed ECMWF pressure and wind field + inverse barometer LF	MOG2D High frequencies forced with analysed ECMW F pressure and wind field (Carrère and Lyard, 2003) (operational version 3.2.0) + inverse barometer Low frequencies		TUGO High frequencies forced with analysed ERA 5 pressure an d wind field + inverse barometer Low frequencies	TUGO High frequencies forced with analysed ER A 5 pressure and wind field ; and after 02/2016 MO G2D High frequencies forced with analysed ECMWF pressure and wind field + inverse barometer Low frequencies		MOG2D High frequencies forced with analysed ECMWF pressure and wind field (Carrère and Lyard, 2003) (operational version 3.2.0) + inverse barometer Low frequencies
MEAN SEA SURFACE	Mean profile	Mean profile for repetitive orbit phases; Hybrid MSS (SIO,CNES/CLS15,DTU15) for geodetic/LOR phase		Mean profile	Mean profile for repetitive orbit phases; Hybrid MSS (SIO, CNES/CLS15,DTU15) for geodetic phase	Mean profile	Mean profile for repetitive orbit phases; Composite MSS (SIO,CNES/CLS15,DTU15) for geodetic/drifting phase		Mean profile	Hybrid MSS (SIO,CNES/CLS15, DTU15)	Hybrid MSS (SIO,CNES/CLS15,DTU15)			

Appendix B

Table B1. List of the 213 tide gauge records with their location and time period analysed. Bold stations indicate the tide gauge sites from the subset covering the 20-year period spanning from January 2000 to December 2019 listed in Table B2.

	Station name	Lon (°E)	Lat (°N)	Period analysed		Station name	Lon (°E)	Lat (°N)	Period analysed
1	Bagenkop	10.68	54.75	11/2006 - 05/2020	52	**Ratan**	**20.90**	**63.99**	**01/1993 - 05/2020**
2	Bandholm	11.48	54.83	01/2014 - 05/2020	53	Ringhals	12.11	57.25	01/1993 - 05/2020
3	Barhoeft	13.03	54.44	01/2011 - 05/2020	54	Rodby	11.35	54.65	01/2005 - 05/2020
4	**Barseback**	**12.9**	**55.76**	**01/1993 - 05/2020**	55	Rodvig	12.37	55.25	01/1993 - 05/2020
5	Bogense	10.08	55.57	01/2014 - 05/2020	56	Rohukula	23.42	58.90	12/2009 - 12/2019
6	Dragor	12.68	55.60	07/2011 - 05/2020	57	Roskilde	12.08	55.65	12/2011 - 05/2020
7	Drogden	12.71	55.54	01/1993 - 05/2020	58	Rostock	12.15	54.08	01/2011 - 05/2020
8	Eckernfoerde	9.84	54.47	01/2011 - 05/2020	59	**Simrishamn**	**14.36**	**55.56**	**01/1993 - 05/2020**
9	Faaborg	10.25	55.10	01/2014 - 05/2020	60	SjaellandsOdde	11.37	55.97	01/1993 - 05/2020
10	**Forsmark**	**18.21**	**60.41**	**01/1993 - 05/2020**	61	Skagen	10.59	57.72	04/1993 - 09/2018
11	Fredericia	9.75	55.57	01/2005 - 05/2020	62	Skagsudde	19.01	63.19	10/1993 - 05/2020
12	**Furuogrund**	**21.23**	**64.92**	**01/1993 - 05/2020**	63	**Skanor**	**12.83**	**55.42**	**01/1993 - 07/2018**
13	Gedser	11.93	54.57	03/1993 - 05/2020	64	**Smogen**	**11.22**	**58.35**	**01/1993 - 05/2020**
14	GoteborgAgnesberg	12.01	57.79	01/2013 - 05/2020	65	Sonderborg	9.78	54.92	01/2014 - 05/2020
15	GoteborgEriksberg	11.91	57.70	01/2013 - 05/2020	66	**Spikarna**	**17.53**	**62.36**	**01/1993 - 05/2020**
16	GoteborgLarjeholm	12.01	57.77	01/2013 - 05/2020	67	**Stenungsund**	**11.83**	**58.09**	**01/1993 - 05/2020**
17	GoteborgTingstadstunneln	11.99	57.72	01/2013 - 05/2020	68	**Stockholm**	**18.08**	**59.32**	**01/1993 - 05/2020**
18	**GoteborgTorshamnen**	**11.79**	**57.68**	**01/1993 - 05/2020**	69	Stralsund	13.10	54.32	01/2011 - 05/2020
19	Greifswald	13.45	54.09	01/2011 - 05/2020	70	Tallinn	24.76	59.44	11/2005 - 05/2020
20	Grena	10.93	56.41	01/1993 - 05/2020	71	TimmendorfPoel	11.38	53.99	01/2011 - 05/2020
21	**Hanko**	**22.98**	**59.82**	**01/1993 - 05/2020**	72	Travemuende	10.87	53.96	01/2005 - 05/2020
22	Heiligenhafen	11.01	54.37	01/2011 - 05/2020	73	Uddevalla	11.89	58.35	12/2010 - 05/2020
23	Holbaek	11.72	55.72	12/2011 - 05/2020	74	Ueckermuende	14.07	53.75	01/2011 - 05/2020
24	Hov	10.27	55.92	12/2011 - 05/2020	75	Vedbaek	12.57	55.85	12/2011 - 05/2020
25	Juelsminde	10.02	55.72	12/1996 - 05/2020	76	**Viken**	**12.58**	**56.14**	**01/1993 - 05/2020**
26	Kalix	23.10	65.70	01/1993 - 05/2020	77	Virtsu	23.51	58.58	12/2009 - 05/2020
27	Kalkgrund	9.89	54.82	01/2011 - 05/2020	78	**Visby**	**18.28**	**57.64**	**01/1993 - 05/2020**
28	Kalvehave	12.17	55.00	01/2014 - 05/2020	79	Wismar	11.46	53.90	01/2011 - 05/2020
29	Kappeln	9.94	54.66	01/2011 - 05/2020	80	Wolgast	13.77	54.04	01/2011 - 05/2020
30	Karrebaeksminde	11.65	55.18	01/2014 - 05/2020	81	**BrestTG**	**-4.50**	**48.38**	**01/1993 - 05/2020**
31	Kelnase	25.01	59.64	02/2017 - 05/2020	82	CherbourgTG	-1.64	49.65	01/1993 - 05/2020
32	KielHoltenau	10.16	54.37	01/2005 - 05/2020	83	ConcarneauTG	-3.91	47.87	06/1999 - 05/2020
33	KielLTG	10.27	54.50	01/2011 - 05/2020	84	LaRochelleTG	-1.23	46.15	10/1995 - 05/2020
34	Koege	12.20	55.45	01/2012 - 05/2020	85	LeConquetTG	-4.78	48.36	01/1993 - 05/2020
35	Koserow	14,00	54.06	11/2005 - 11/2019	86	LeHavreTG	0.11	49.48	01/1993 - 05/2020
36	Kristineberg1	11.45	58.25	04/2012 - 05/2020	87	MarseilleTG	5.35	43.28	10/1998 - 05/2020
37	**Kungsholmsfort**	**15.59**	**56.11**	**01/1993 - 05/2020**	88	MonacoTG	7.42	43.73	04/1999 - 05/2020
38	**Kungsvik**	**11.13**	**59.00**	**01/1993 - 05/2020**	89	NiceTG	7.29	43.70	03/1998 - 05/2020
39	LandsortNorra	17.86	58.77	10/2004 - 05/2020	90	RoscoffTG	-3.97	48.72	01/1993 - 05/2020
40	Langballigau	9.65	54.82	01/2011 - 05/2020	91	SaintGildasTG	-2.25	47.14	02/1993 - 06/2017
41	Leppneeme	24.87	59.55	02/2017 - 05/2020	92	**SaintMaloTG**	**-2.03**	**48.64**	**08/1993 - 04/2020**
42	Luebeck	10.70	53.89	01/2011 - 05/2020	93	ToulonTG	5.91	43.12	01/1993 - 05/2020
43	Marviken	16.84	58.55	01/1993 - 09/2019	94	Aberdeen	-2.08	57.15	01/1993 - 05/2020
44	Munalaiu	24.12	58.23	02/2016 - 05/2020	95	AlcudiaTG	3.14	39.83	09/2009 - 05/2020
45	Neustadt	10.81	54.10	01/2011 - 05/2020	96	AlgecirasTG	-5.40	36.18	07/2009 - 05/2020
46	**OlandsNorraUdde**	**17.10**	**57.37**	**01/1993 - 05/2020**	97	AlmeriaTG	-2.48	36.83	01/2006 - 05/2020
47	Onsala	11.92	57.39	06/2015 - 05/2020	98	Aranmore	-8.50	54.99	05/2008 - 05/2020
48	**Oskarshamn**	**16.48**	**57.28**	**01/1993 - 05/2020**	99	ArklowHarbur	-6.15	52.79	08/2003 - 05/2020
49	Paldiski	24.08	59.33	10/2006 - 05/2020	100	Ballycotton	-8,00	51.83	10/2010 - 05/2020
50	**Pori**	**21.46**	**61.59**	**01/1993 - 05/2020**	101	Ballyglass	-9.89	54.25	05/2008 - 04/2020
51	Porvoo	25.63	60.21	08/2014 - 05/2020	102	Bangor	-5.67	54.67	11/1994 - 05/2020

	Station name	Lon (°E)	Lat (°N)	Period analysed		Station name	Lon (°E)	Lat (°N)	Period analysed
103	**BarcelonaTG**	**2.16**	**41.34**	**01/1993 - 05/2020**	162	AlteWeserTG	8.13	53.86	01/2014 - 05/2020
104	Barmouth	-4.03	52.72	01/1993 - 05/2020	163	AndenesTG	16.13	69.33	01/2014 - 05/2020
105	**BilbaoTG**	**-3.05**	**43.36**	**01/1993 - 05/2020**	164	AWGTG	5.94	53.49	06/2015 - 05/2020
106	BonanzaTG	-6.34	36.80	01/1993 - 05/2020	165	BergenTG	5.32	60.40	01/2007 - 05/2020
107	Bournemouth	-1.87	50.71	06/1996 - 05/2020	166	BodoeTG	14.39	67.29	01/2007 - 05/2020
108	CarbonerasTG	-1.90	36.97	07/2013 - 05/2020	167	BorkumTG	6.75	53.56	01/2014 - 05/2020
109	Castletownbere	-9.90	51.65	12/2006 - 05/2020	168	Brouwershavensegat8TG	3.62	51.77	08/2014 - 12/2019
110	CorunaTG	-8.39	43.36	01/1993 - 05/2020	169	CadzandTG	3.38	51.38	08/2014 - 12/2019
111	Dundalk	-6.39	54.01	04/2008 - 01/2013	170	DenHelderTG	4.75	52.97	01/2014 - 12/2019
112	Felixstowe	1.35	51.97	01/1993 - 01/2011	171	EemshavenTG	6.84	53.46	08/2014 - 05/2020
113	Fenit	-9.86	52.27	01/2007 - 05/2020	172	EuroplatformTG	3.28	52.00	01/2014 - 12/2019
114	Ferrol2TG	-8.25	43.48	01/2007 - 05/2020	173	F3platformTG	4.72	54.85	08/2014 - 12/2019
115	FerrolTG	-8.33	43.46	01/2007 - 05/2020	174	HammerfestTG	23.68	70.66	01/2014 - 05/2020
116	Fishguard	-4.98	52.02	01/1993 - 05/2020	175	HanstholmTG	8.60	57.12	01/2015 - 05/2020
117	FormenteraTG	1.42	38.73	09/2009 - 05/2020	176	HarstadTG	16.55	68.80	01/2014 - 05/2020
118	GandiaTG	-0.15	38.99	07/2007 - 05/2020	177	HavnebyTG	8.57	55.09	01/2015 - 05/2020

119	GijonTG	-5.70	43.56	07/1995 - 05/2020
120	Hinkley	-3.13	51.22	01/1993 - 05/2020
121	Holyhead	-4.62	53.32	02/2005 - 05/2020
122	Howth	-6.07	53.39	10/2006 - 11/2019
123	**HuelvaTG**	**-6.83**	**37.13**	**09/1996 - 05/2020**
124	IbizaTG	1.45	38.91	01/2003 - 05/2020
125	Ilfracombre	-4.12	51.22	01/1993 -05/2020
126	Kinlochbervie	-5.05	58.46	01/1993 - 05/2020
127	LangosteiraTG	-8.53	43.35	01/2014 - 05/2020
128	Leith	-3.18	55.99	01/1993 - 05/2020
129	Llandudno	-3.82	53.31	05/2014 - 05/2020
130	Lowestoft	1.75	52.47	01/1993 - 05/2020
131	MahonTG	4.27	39.89	10/2009 - 05/2020
132	**MalagaTG**	**-4.42**	**36.71**	**01/1993 - 05/2020**
133	MarinTG	-8.69	42.41	01/2010 - 05/2020
134	MelillaTG	-2.92	35.29	10/2007 - 05/2020
135	Milford	-5.05	51.72	01/1993 - 05/2020
136	Millport	-4.90	55.75	01/1993 - 05/2020
137	MotrilTG	-3.52	36.72	01/2005 - 05/2020
138	Newhaven	0.07	50.78	01/1993 - 05/2020
139	Newlyn	-5.53	50.10	01/1993 - 09/2018
140	NorthShields	-1.43	55.00	01/1993 - 05/2020
141	PalmadeMallorcaTG	2.64	39.56	09/2009 - 05/2020
142	Plymouth	-4.19	50.37	01/1993 - 05/2020
143	PortEllen	-6.19	55.63	01/1993 - 02/2011
144	Portpatrick	-5.12	54.84	01/1993 - 05/2020
145	Portrush	-6.67	55.20	07/1995 - 05/2020
146	Portsmouth	-1.11	50.80	01/1993 - 05/2020
147	RingaskiddyNMCI	-8.30	51.84	01/2012 - 05/2020
148	RossaveelPier	-9.56	53.27	09/2020 - 05/2020
149	SaguntoTG	-0.21	39.63	07/2006 - 05/2020
150	**SantanderTG**	**-3.79**	**43.46**	**01/1993 - 05/2020**
151	StHelier	-2.12	49.18	01/1993 - 05/2020
152	Stornoway	-6.38	58.22	01/1993 - 05/2020
153	TarifaTG	-5.60	36.01	07/2009 - 05/2020
154	TarragonaTG	1.21	41.08	05/2011 - 05/2020
155	Tobermory	-6.06	56.62	03/1993 - 05/2020
156	**ValenciaTG**	**-0.33**	**39.46**	**01/1993 - 05/2020**
157	VigoTG	-8.73	42.24	01/1993 - 05/2020
158	Weymouth	-2.45	50.61	01/1993 - 05/2020
159	Wick	-3.08	58.43	01/1993 - 05/2020
160	ANDRATX	2.39	39.55	06/2011 - 05/2020
161	AalesundTG	6.15	62.47	01/2007 - 05/2020
178	HelgeroaTG	9.86	59,00	01/2007 - 05/2020
179	HelgolandTG	7.89	54.18	01/2014 - 05/2020
180	HirtshalsTG	9.97	57.60	01/2015 - 05/2020
181	HoekVanHollandTG	4.12	51.98	01/2014 - 12/2019
182	HoernumTG	8.30	54.76	01/2014 - 05/2020
183	HonningsvaagTG	25.97	70.98	01/2007 - 05/2020
184	HuibertgatTG	6.40	53.57	06/2014 - 12/2019
185	IJmondstroompaalTG	4.52	52.46	08/2014 - 05/2020
186	K141TG	3.63	53.27	06/2015 - 05/2020
187	KabelvaagTG	14.48	68.21	01/2007 - 05/2020
188	KristiansundTG	7.73	63.11	01/2007 - 05/2020
189	L91TG	4.87	53.57	06/2015 - 05/2020
190	LauwersoogTG	6.20	53.41	06/2015 - 12/2019
191	LichteilandGoeree1TG	3.67	51.93	01/2015 - 05/2020
192	ListTG	8.44	55.02	01/2014 - 09/2018
193	MaloyTG	5.11	61.93	01/2007 - 05/2020
194	MandoTG	8.58	55.28	01/2015 - 05/2020
195	NieuwpoortTG	2.73	51.15	08/2014 - 05/2020
196	NorderneyTG	7.16	53.70	01/2014 - 05/2020
197	NorthCormorantTG	1.16	61.34	08/2014 - 05/2020
198	OostendeTG	2.93	51.23	08/2014 - 05/2020
199	OscarsborgTG	10.60	59.68	01/2007 - 05/2020
200	RorvikTG	11.23	64.86	01/2007 - 05/2020
201	StavangerTG	5.73	58.97	01/2014 - 05/2020
202	ThyboronKystTG	8.21	56.71	01/2015 - 05/2020
203	TorsmindeKystTG	8.12	56.37	01/2015 - 05/2020
204	TregdeTG	7.55	58.01	01/2007 - 05/2020
205	TromsoeTG	18.96	69.65	01/2007 - 05/2020
206	VardoeTG	31.10	70.37	01/2014 - 05/2020
207	VikerTG	10.95	59.04	01/2007 - 05/2020
208	VlakteVdRaanTG	3.24	51.50	08/2014 - 05/2020
209	VlielandHavenTG	5.09	53.30	08/2014 - 05/2020
210	WangeroogeTG	7.93	53.81	01/2014 - 05/2020
211	WestkapelleTG	3.44	51.52	08/2014 - 05/2020
212	WilhelmshavenTG	8.15	53.51	01/2014 - 05/2020
213	ZeebruggeTG	3.20	51.35	08/2014 - 05/2020

Table B2. Tide gauge stations from the subset covering the 20-year period spanning from January 2000 to December 2019 located in the Baltic and Mediterranean Seas, and along the North Atlantic European shore. The location of the tide gauge sites, the linear trend (mm year^{-1}) computed from the DUACS DT2021 and DT2018 reprocessing *all satellites* and *two satellites* most correlated altimeter grid point to tide gauges, the tide gauges, and the mean trend value are displayed.

Station		Longitude (°E)	Latitude (°N)	Trend DT2021 all satellites (mm year^{-1})	Trend DT2021 two satellites (mm year^{-1})	Trend DT2018 all satellites (mm year^{-1})	Trend DT2018 two satellites (mm year^{-1})	Trend TG (mm year^{-1})
Barseback	Baltic Sea	12.90	55.76	3.22	3.26	2.99	2.88	2.60
Forsmark		18.21	60.41	3.49	3.53	3.71	3.03	1.12
Furuogrund		21.23	64.92	3.33	3.07	3.45	2.82	2.62
GoteborgTorshamnen		11.79	57.68	3.62	3.70	3.84	3.56	2.31
Hanko		22.98	59.82	2.33	2.81	2.88	2.72	0.16
Kungsholmsfort		15.59	56.11	3.12	2.87	3.19	2.37	2.96
Kungsvik		11.13	59.00	3.52	3.50	3.70	3.60	1.72
OlandsNorraUdde		17.10	57.37	3.10	3.03	3.18	2.58	0.69
Oskarshamn		16.48	57.28	3.02	3.05	3.24	2.50	1.27
Pori		21.46	61.59	4.11	3.64	4.35	3.50	4.34
Ratan		20.90	63.99	3.34	3.19	3.48	2.77	2.02
Simrishamn		14.36	55.56	3.12	2.90	3.21	2.65	1.34
Skanor		12.83	55.42	3.43	3.26	3.33	2.83	2.14
Smogen		11.22	58.35	3.23	3.50	3.48	3.50	1.26
Spikarna		17.53	62.36	3.56	3.32	3.75	3.05	0.99
Stenungsund		11.83	58.09	3.63	3.75	3.48	3.49	1.93
Stockholm		18.08	59.32	3.02	3.23	3.37	3.01	1.26
Viken		12.58	56.14	3.21	3.42	3.22	3.10	1.51
Visby		18.28	57.64	3.13	2.80	3.35	2.70	0.73
Brest	North Atlantic European Shore	-4.50	48.38	2.57	2.61	2.68	2.57	2.64
SaintMalo		-2.03	48.64	1.26	2.59	1.60	2.54	2.37
Bilbao		-3.05	43.36	2.63	2.36	2.40	2.10	2.94
Huelva		-6.83	37.13	3.30	3.39	3.05	2.85	2.27
Santander		-3.79	43.46	2.33	2.42	2.51	2.12	1.88
Barcelona	Med Sea	2.16	41.34	3.33	3.25	3.07	2,77	5.06
Malaga		-4.42	36.71	3.25	2.58	2.19	2.58	0.77
Valencia		-0.33	39.46	3.62	3.47	3.15	2.84	2.13
Mean value				**3.14**	**3.13**	**3.18**	**2.85**	**1.96**

Data availability

Altimetry datasets are available from the Copernicus Marine Service web portal (https://resources.marine.copernicus.eu/products/, last access: 15 July 2022). Tide gauge measurements are available from the Copernicus Marine INS-TAC data repository web portal (www.marineinsitu.eu, last access: 3 June 2022). Tide gauge data are provided by the following regional in situ data production centres: Puertos del Estado (Spain) for the Iberia-Biscay-Ireland region; HCMR (Greece) for the Mediterranean Sea; IMR (Norway) for the Arctic; SMHI (Sweden) for the Baltic Sea; BSH (Germany) for the North West Shelves region; Coriolis (France) for the global ocean. The ancillary data used to obtain the Dynamic Atmospheric Correction applied to the altimetry grid point closest to the tide gauge locations are available at the AVISO webpage: https://www.aviso.altimetry.fr/en/ (last access: 16 May 2022).

Author contributions

Conceptualisation: Antonio Sánchez Román, M. Isabelle Pujol, Ananda Pascual and Yannice Faugère; altimetry data processing: M. Isabelle Pujol; tide gauge data processing: Antonio Sánchez Román; statistical analysis: Antonio Sánchez Román and Ananda Pascual; manuscript writing: Antonio Sánchez Román, with inputs from all co-authors. All authors have read and agreed to the published version of the manuscript.

Competing interests

The authors declare that they have no conflict of interest

Acknowledgement

This study has been conducted in the frame of the Copernicus Marine Service SL-TAC and In Situ TAC (INS-TAC) projects. The Copernicus Marine Service, led by Mercator-Ocean, is based on a distributed model of service production, relying on the expertise of a wide network of participating European organisations involved in operational oceanography. We acknowledge the regional in situ data production centres responsible for the collection and distribution of the tide gauge data used in this study: Puertos del Estado (Spain) for the Iberia-Biscay-Ireland region; HCMR (Greece) for the Mediterranean Sea; IMR (Norway) for the Arctic; SMHI (Sweden) for the Baltic Sea; BSH (Germany) for the North-West Shelves region; Coriolis (France) for the global ocean. This work represents a contribution to CSIC Interdisciplinary Thematic Platform (PTI) Teledetección. (PTI-TELEDETECT) and it was carried out within the framework of the activities of the Spanish Government through the "Maria de Maeztu Centre of Excellence" accreditation to IMEDEA (CSIC-UIB) (CEX2021-001198).

References

Ablain, M. and Legeais, J. F.: SLOOP Tache 2.4 : Amélioration du filtrage de la correction ionospherique bifréquence, 2010.

Agha Karimi A, Bagherbandi M and Horemuz M.: Multidecadal Sea Level Variability in the Baltic Sea and Its Impact on Acceleration Estimations, Front. Mar. Sci. 8:702512, https://doi.org/10.3389/fmars.2021.702512 , 2021.

Andersen O., Stenseng, L., Piccioni, G., Knudsen. P.: The DTU15 MSS (Mean Sea Surface) and DTU15LAT (Lowest Astronomical Tide) reference surface. ESA Living Planet Symposium 2016 - Prague, Czech Republic. http://lps16.esa.int/page_session189.php#1579p, 2016.

Aulicino, G., Y. Cotroneo, S. Ruiz, A. J. Sánchez Román, A. Pascual, G. Fusco, J. Tintoré, G. Budillon. Monitoring the Algerian Basin through glider observations, satellite altimetry and numerical simulations along a SARAL/AltiKa track. Journal of Mar. Sys. 179, 55-71, 2018.

Ballarotta, M., Ubelmann, C., Pujol, M.-I., Taburet, G., Fournier, F., Legeais, J.-F., Faugère, Y., Delepoulle, A., Chelton, D., Dibarboure, G., and Picot, N.: On the resolutions of ocean altimetry maps, Ocean Sci., 15, 1091–1109, https://doi.org/10.5194/os-15-1091-2019, 2019.

Barceló-Llull B, Pascual A, Sánchez-Román A, Cutolo E, d'Ovidio F, Fifani G, Ser-Giacomi E, Ruiz S, Mason E, Cyr F, Doglioli A, Mourre B, Allen JT, Alou-Font E, Casas B, Díaz-Barroso L, Dumas F, Gómez-Navarro L and Muñoz C. Fine-Scale Ocean Currents Derived From in situ Observations in Anticipation of the Upcoming SWOT Altimetric Mission. Front. Mar. Sci. 8:679844. doi: 10.3389/fmars.2021.679844 , 2021.

Birol, F.; Fuller, N.; Lyard, F.; Cancet, M.; Niño, F.; Delebecque, C.; Fleury, S.; Toublanc, F.; Melet, A.; Saraceno, M.; et al. Coastal applications from nadir altimetry: Example of the X-TRACK regional products. Adv. Space Res., 59, 936–953, 2017.

Birol, F.; Léger, F.; Passaro, M.; Cazenave, A.; Niño, F.; Calafat, F.M.; Shaw, A.; Legeais, J.-F.; Gouzenes, Y.; Schwatke, C.; et al. The X-TRACK/ALES multi-mission processing system: New advances in altimetry towards the coast. Adv. Space Res., 67, 2398–2415, 2021.

Carrère, L., and F. Lyard: Modeling the barotropic response of the global ocean to atmospheric wind and pressure forcing—comparisons with observations. *Geophys. Res. Lett.* 30: 1275. doi: 10.1029/2002GL016473, 2003

Carrere, L., Lyard, F., Allain, D., Cancet, M., Picot, N., Guillot, A., Faugère, Y., Dupuy, S., and Baghi, R.: Final version of the FES2014 global ocean tidal model, which includes a new loading tide solution, OSTST, La Rochelle, France, https://ostst.aviso.altimetry.fr/fileadmin/user_upload/tx_ausyclsseminar/files/Poster_FES2014b_OSTS T_2016.pdf, 2016.

Cartwright, D. E. and Tayler, R. J.: New Computations of the Tide-generating Potential, Geophysical Journal International, 23, 45–73, https://doi.org/10.1111/j.1365-246X.1971.tb01803.x, 1971.

Cartwright, D. E. and Edden, A. C.: Corrected Tables of Tidal Harmonics, Geophysical Journal International, 33, 253–264, https://doi.org/10.1111/j.1365-246X.1973.tb03420.x, 1973.

Cipollini, P., Calafat, F.-M., Jevrejeva, S., Melet, A., Prandi, P.: Monitoring sea level in the coastal zone with satellite altimetry and tide gauges. Surv. Geophys. 2017**,** 38:33–57. https://doi.org/10.1007/s10712-016-9392-0, 2017

Codiga, D.L.: Unified Tidal Analysis and Prediction Using the UTide Matlab Functions. Technical Report 2011-01. Graduate School of Oceanography, University of Rhode Island, Narragansett, RI. 59pp. ftp://www.po.gso.uri.edu/pub/downloads/codiga/pubs/2011Codiga-UTide-Report.pdf, 2011

Desai, S., Wahr, J., and Beckley, B.: Revisiting the pole tide for and from satellite altimetry, J Geod, 89, 1233–1243, https://doi.org/10.1007/s00190-015-0848-7, 2015.

Dibarboure, G., Pujol, M.-I., Briol, F., Le Traon, P.-Y., Larni- col, G., Picot, N., Mertz, F., Escudier, P., Ablain, M., and Dufau, C.: Jason-2 in DUACS: first tandem results and impact on processing and products, Mar. Geod., OSTM Jason-2 Calibration/Validation Special Edition – Part 2, 34, 214–241, doi:10.1080/01490419.2011.584826, 2011.

Dorandeu, J., and P.-Y. Le Traon: Effects of global mean atmospheric pressure variations on mean sea level changes from Topex/Poseidon. J. Atmos. Oceanic Technol. 16: 1279 – 1283, 1999.

Efron, B., and Tibshirani, R.: Bootstrap methods for standart errors, condifence intervals, and other measures of statistical accuracy, Statistical Science, Vol. 1, No. 1: 54 – 77, 1986.

Faugère, Y., Taburet, G., Ballarotta, M., Pujol, I., Legeais, J. F., Maillard, G., Durand, C., Dagneau, Q., Lievin, M., Sanchez Roman, A., and Dibarboure, G.: DUACS DT2021: 28 years of reprocessed sea level altimetry products, EGU General Assembly 2022, Vienna, Austria, 23–27 May 2022, EGU22-7479, https://doi.org/10.5194/egusphere-egu22-7479, 2022.

Fernandes, M. J., Lázaro, C., Ablain, M., and Pires, N.: Improved wet path delays for all ESA and reference altimetric missions, Remote Sensing of Environment, 169, 50–74, https://doi.org/10.1016/j.rse.2015.07.023, 2015.

Fernandes, M. J. and Lázaro, C.: GPD+ Wet Tropospheric Corrections for CryoSat-2 and GFO Altimetry Missions, 8, 851, https://doi.org/10.3390/rs8100851, 2016.

Gaspar, P. and Ogor, F.: Estimation and analysis of the sea state bias of the ERS-1 altimeter, technical report of IFREMER contract 94/2.426016/C, 1994.

Grégoire, M.; EO4SIBS Consortium (ESA Project). Earth Observation Products for Science and Innovation in the Black Sea, Presented at EGU21, Gather Online, 2021. Available online: https://meetingorganizer.copernicus.org/EGU21/EGU21-10237.html (accessed on 12 April 2023).

Heslop, E. E., A. Sánchez-Román, A. Pascual, D. Rodríguez, K.A. Reeve, Y. Faugère, M. Raynal. Sentinel-3A views ocean variability more accurately at finer resolution. Geophy. Res. Letters, 44, 1-8, 2017.

Iijima, B. A., Harris, I. L., Ho, C. M., Lindqwister, U. J., Mannucci, A. J., Pi, X., Reyes, M. J., Sparks, L. C., and Wilson, B. D.: Automated daily process for global ionospheric total electron content maps and satellite ocean altimeter ionospheric calibration based on Global Positioning System data, Journal of Atmospheric and Solar-Terrestrial Physics, 61, 1205–1218, https://doi.org/10.1016/S1364- 6826(99)00067-X, 1999.

International Altimetry Team*.Altimetry for the future: Building on 25 years of progress. Advances in Space Research, 68(2), 319-363, https://doi.org/10.1016/j.asr.2021.01.022, 2021.

Jousset, S. and Mulet: New Mean Dynamic Topography of the Black Sea and Mediterranean Sea from altimetry, gravity and in-situ data, 2020.

Jousset, S., Aydogdu, A., Ciliberti, S., Clementi, E., Escudier, R., Jansen, E., Lima, L., Menna, M., Mulet, S., Nigam, T., Sanchez-Roman, A., Tarry, D. R., Pascual, A., Peneva, E., Poulain, P.-M., and Taupier- Letage, I.: New Mean Dynamic Topography of the Mediterranean Sea from altimetry, gravity and in- situ data, 2022 (in preparation).

Laíz, I., Gómez-Enri, J., Tejedor, B., Aboitiz, A., Villares, P.: Seasonal sea level varia- tions in the gulf of Cadiz continental shelf from in-situ measurements and satellite altimetry. Cont. Shelf Res. 53, 77–88, http://dx.doi.org/10.1016/j.csr.2012.12.008, 2013.

Laíz, I., Tejedor, B., Gómez-Enri, J., Aboitiz, A., Villares, P.: Contributions to the sea level seasonal cycle within the Gulf of Cadiz (Southwestern Iberian Peninsula). J. Mar. Syst. 159, 55-66, https://doi.org/10.1016/j.jmarsys.2016.03.006, 2016.

Marcos, M., Pascual, A., and Pujol, I.: Improved satellite altimeter mapped sea level anomalies in the Mediterranean Sea: A comparison with tide gauges, Advances in Space Research 56, 596 – 604, https://doi.org/10.1016/j.asr.2015.04.027, 2015.

Mercier, F.; Rosmorduc, V.; Carrere, L.; Thibaut, P. Coastal and Hydrology Altimetry Product (PISTACH) Handbook. 2010. Available online: https://www.aviso.altimetry.fr/fileadmin/documents/data/tools/hdbk_Pistach.pdf (accessed on 12 April 2023).

Mertz, F., Mercier, F., Labroue, S., Tran, N., and Dorandeu, J.: ERS-2 OPR data quality assessment ; Long-term monitoring - particular investigation, 2005.

Morrow R, Fu LL, Ardhuin F, Benkiran M, Chapron B, Cosme E, d'Ovidio F, Farrar JT, Gille ST, Lapeyre G, Le Traon P-Y, Pascual A, Ponte A, Qiu B, Rascle N, Ubelmann C, Wang J, Zaron E. Global observations of fine-scale ocean surface topography with the surface water and ocean topography (SWOT) mission. Front Mar Sci. https://doi.org/10.3389/fmars.2019.0023, 2019.

Morrow, R., Fu, LL., Rio, MH. *et al.* Ocean Circulation from Space. Surv Geophys. https://doi.org/10.1007/s10712-023-09778-9, 2023.

Mulet, S., Rio, M.-H., Etienne, H., Artana, C., Cancet, M., Dibarboure, G., Feng, H., Husson, R., Picot, N., Provost, C., and Strub, P. T.: The new CNES-CLS18 global mean dynamic topography, 17, 789–808, https://doi.org/10.5194/os-17-789-2021, 2021.

Pascual, A.; Faugère, Y.; Larnicol, G.; Le Traon, P.-Y.: Improved description of the ocean mesoscale variability by combining four satellite altimeters. Geophys. Res. Lett., *33*, L02611, 2006.

Pascual, A., Marcos, M., Gomis, D.: Comparing the sea level response to pressure and wind forcing of two barotropic models: validation with tide gauge and altimetry data. J. Geophys. Res. 113, C07011, http://dx.doi.org/10.1029/2007jc004459 , 2008

Pascual, A., Boone, C., Larnicol, G., Le Traon, P.Y.: On the quality of real-time altimeter gridded fields: comparison with in situ data. J. Atmos. Ocean. Technol. 2009, 26, 556–569. https://doi.org/10.1175/2008JTECHO556.1, 2009.

Pascual, A., Lana, A., Troupin, C., Ruiz, S., Faugère, Y., Escudier R., and Tintoré, J. Assessing SARAL/AltiKa Data in the Coastal Zone: Comparisons with HF Radar Observations, Marine Geodesy, 38:sup1, 260-276, DOI: 10.1080/01490419.2015.1019656, 2015.

Peltier W.R.: Postglacial Variations in the Level of the Sea: Implications for Climate Dynamics and Solid-Earth Geophysics. Reviews of Geophysics 1998. 36(4),603-689, 1998.

Peltier W.R.: Global Glacial Isostasy and the Surface of the Ice-Age Earth: The ICE-5G(VM2) model and GRACE. Ann. Rev. Earth. Planet. Sci. 2004. 32,111-149, 2004.

PSMSL. Permanent Service for Mean Sea Level: "Tide Gauge Data". 2016. Available online: http:

//www.psmsl.org/data/obtaining/ (accessed on 4 July 2022).

PUGS document of the sea level products version vDT2021 D3.SL.1-v2.0_PUGS_of_v2DT2021_SeaLevel_products_v1.1, 2021. Available online: https://datastore.copernicus-climate.eu/documents/satellite-sea-level/vDT2021/D3.SL.1-v2.0_PUGS_of_v2DT2021_SeaLevel_products_v1.1_APPROVED_Ver1.pdf (accessed on 4 July 2022).

Pujol, M., Schaeffer, P., Faugère, Y., Raynal, M., Dibarboure, G., and Picot, N.: Gauging the Improvement of Recent Mean Sea Surface Models: A New Approach for Identifying and Quantifying Their Errors, J. Geophys. Res. Oceans, 123, 5889–5911, https://doi.org/10.1029/2017JC013503, 2018

Pujol, M.-I.; Dupuy, S.; Vergara, O.; Sánchez Román, A.; Faugère, Y.; Prandi, P.; Dabat, M.-L.; Dagneaux, Q.; Lievin, M.; Cadier, E.; et al. Refining the Resolution of DUACS Along-Track Level-3 Sea Level Altimetry Products. Remote

Sens.,15,793. https:// doi.org/10.3390/rs15030793, 2023.

QUID document for Sea Level TAC DUACS products CMEMS-SL-QUID-008-032-068, 2022. Available online: https://catalogue.marine.copernicus.eu/documents/QUID/CMEMS-SL-QUID-008-032-068.pdf (accessed on 4 July 2022).

Ries, J. C. and Desai, S.: Conventional model update for rotational deformation, 2017.

Roblou, L.; Lamouroux, J.; Bouffard, J.; Lyard, F.; Le Hénaff, M.; Lombard, A.; Marsaleix, P.; De Mey, P.; Birol, F. Post-processing altimeter data towards coastal applications and integration into coastal models. In *Coastal Altimetry*; Vignudelli, S., Kostianoy, A., Cipollini, P., Benveniste, J., Eds.; Springer: Berlin/Heidelberg, Germany, 2011; pp. 217–246.

Sánchez-Román, A., Ruiz, S., Pascual, A., Mourre, B., and Guinehut, S.: On the mesoscale monitoring capability of Argo floats in the Mediterranean Sea, Ocean Sci., 13, 223–234, https://doi.org/10.5194/os-13-223-2017, 2017.

Sánchez-Román, A.; Pascual, A.; Pujol, M.-I.; Taburet, G.; Marcos, M.; Faugère, Y.: Assessment of DUACS Sentinel-3A Altimetry Data in the Coastal Band of the European Seas: Comparison with Tide Gauge Measurements. Remote Sens. 2020, *12*, 3970, https://doi.org/10.3390/rs12233970, 2020.

Sandwell D., Schaeffer P., Dibarboure G., Picot N.: High Resolution Mean Sea Surface for SWOT. https://spark.adobe.com/page/MkjujdFYVbHsZ/, 2017.

Scharroo, R. and Smith, W. H. F.: A global positioning system–based climatology for the total electron content in the ionosphere, 115, https://doi.org/10.1029/2009JA014719, 2010.

Taibi, H., Haddad, M.: Estimating trends of the Mediterranean Sea level changes from tide gauge and satellite altimetry data (1993–2015). *J.* Ocean. Limnol. **37**, 1176–1185. https://doi.org/10.1007/s00343-019-8164-3, 2019.

Tran, N., Labroue, S., Philipps, S., Bronner, E., and Picot, N.: Overview and Update of the Sea State Bias Corrections for the Jason-2, Jason-1 and TOPEX Missions, 33, 348–362, https://doi.org/10.1080/01490419.2010.487788, 2010.

Tran, N., Philipps, S., Poisson, J.-C., Urien, S., Bronner, E., and Picot, N.: Impact of GDR_D standards on SSB corrections, OSTST, Venice, Italie, http://www.aviso.altimetry.fr/fileadmin/documents/OSTST/2012/oral/02_friday_28/01_instr_processing_I/01_IP1_Tran.pdf, 2012.

Tran, N.: Rapport Annuel d'activité SALP - Activité SSB, 2015.

Tran, N.: Envisat ESL Phase-F: Tuning activities for Envisat reprocessing baseline v3.0 (Wind, SSB, Rain and Ice), 2017.

Tran, N.: ESL Cryosat-2: Tuning activities: wind speed and SSB, 2018.

Tran, N.: Rapport Annuel d'activité SALP - Activité SSB, 2019.

Valladeau ,G., Legeais, J. F., Ablain, M., Guinehut, S., and Picot, N.: Comparing Altimetry with Tide Gauges and Argo Profiling Floats for Data Quality Assessment and Mean Sea Level Studies, Marine Geodesy, 35:sup1, 42-60, DOI: 10.1080/01490419.2012.718226, 2012.

Vignudelli, S., Birol, F., Benveniste, J., Fu, L.-L, Picot, N., Raynal, M., and Roinard, H.: Satellite Altimetry Measurements of Sea Level in the Coastal Zone. Surv. Geophys. 40. 1319–1349. https://doi.org/10.1007/s10712-019-09569-1, 2019.

Von Schuckmann, K., Le Traon, P.-Y., Smith, N., Pascual, A., Brasseur, P.; Fennel, K., Djavidnia, S., Aaboe, S., Fanjul, E.A., Autret, E., et al.: Copernicus Marine Service Ocean State Report. J. Oper. Ocean., 11, S1–S142, 2018.

Wöppelmann, G.; Marcos, M.: Vertical land motion as a key to understanding sea level change and variability. Rev. Geophys., 54, 64–92, https://doi.org/10.1002/2015RG000502, 2016.

Zaron, E. D.: Baroclinic Tidal Sea Level from Exact-Repeat Mission Altimetry, 49, 193–210, https://doi.org/10.1175/JPO-D-

18-0127.1, 2019.